

Complete stabilization and improvement of the characteristics of tunnel junctions by thermal annealing

P. J. Koppinen, L.M. Väistö, and I.J. Maasilta

Nanoscience Center, Department of Physics, University of Jyväskylä,

P. O. Box 35, FIN-40014 University of Jyväskylä, Finland.

(Dated: February 6, 2008)

We have observed that submicron sized Al-AlO_x-Al tunnel junctions can be stabilized completely by annealing them in vacuum at temperatures between 350°C and 450°C. In addition, low temperature characterization of the samples after the annealing treatment showed a marked improvement of the tunneling characteristics due to disappearance of unwanted resonances in the current. Charging energy, tunneling resistance, barrier thickness and height all increase after the treatment. The superconducting gap is not affected, but supercurrent is reduced in accordance with the increase of tunneling resistance.

Submicron sized metal-insulator-metal (MIM) tunnel junctions have been used widely in applications such as radiation detectors[1], single electron transistors (SET)[2], and tunnel junction coolers and thermometers [3]. They are also the central element in superconducting quantum bits [4, 5, 6, 7, 8], and magnetic junctions [9] are developed for memory applications. However, there are often problems with stability of the junctions in room air conditions, the most noticeable being aging, i.e. a slowly creeping increase of the tunneling resistance R_T with time. Instability of the junctions is an obvious drawback when considering practical and commercial applications of tunnel junctions.

One possible reason for aging is the absorption of unwanted molecules into the barrier. Direct knowledge of these processes is sketchy, although it is known that vacuum conditions can slow down aging significantly. [10] Another possibility is the relaxation of the oxide barrier properties. Typically, tunnel barriers in MIM junctions are fabricated by room temperature thermal oxidation of a disordered base electrode. This procedure results in formation of a polycrystalline or amorphous oxide layer, in which atoms are not in their global equilibrium positions. The relaxation from this "glassy" state could take months at room temperature. Moreover, in AlO_x barriers studied here, chemisorbed oxygen ions bound on the barrier surface during fabrication have also been shown to be a source of instabilities. [11]

A typical remedy for finding a better energy minimum is thermal annealing, the artificial acceleration of the relaxation processes by heating up the sample for some time and then letting it cool again. For technologically important Nb/Al-AlO_x/Nb junctions, annealing treatments in gas atmospheres (He, N₂, Ar, air) were shown to change the barrier properties, always increasing R_T . [12, 13, 14, 15] On the other hand, for magnetic tunnel junctions, improvements in their performance were obtained with vacuum anneals. [16, 17]

In this letter we discuss how Al-AlO_x-Al tunnel junctions can be completely stabilized, and their characteristics improved by thermal annealing in vacuum. The general trend of increase of R_T with the annealing is re-

produced. The bias voltage dependence of the tunneling conductance reveal that the junction characteristics become more ideal after the anneal. In addition, the charging energy, the effective barrier thickness and height all increase due to the annealing. Previous work on annealed Al-AlO_x-Al junctions [18] is partly inconsistent with our results, which is not surprising, as they used a forming gas (H₂/N₂) atmosphere in their process instead of the inert vacuum used here.

A total number of 178 Al-AlO_x-Al samples were annealed, containing either a single junction or two junctions in series, fabricated by conventional electron beam (e-beam) and standard double angle vacuum evaporation techniques. All the junctions had either a junction area $\sim 0.05\mu\text{m}^2$ or $\sim 0.15\mu\text{m}^2$. All samples were fabricated on oxidized silicon substrates, which were usually cleaned with an oxygen plasma just before Al deposition. For a few samples which were not annealed, plasma cleaning was not performed to see how the aging process is affected. The 300 nm wide and 55 nm thick Al wires were e-beam evaporated in high vacuum at a rate 0.3 nm/s, and the AlO_x barriers were thermally grown *in situ* in pure oxygen at ~ 0.2 -0.5 mbar for 3 – 5 minutes. To reduce the effects of contamination, all samples were post-oxidized *in situ* as a last step in ~ 0.5 bar of pure oxygen for five minutes. The samples were annealed in a vacuum chamber ($P < 10^{-3}$ mbar) to temperatures ranging from 200°C to 500°C. The temperature cycle consisted of a quick (minutes) heating phase followed by a slow (hours) cooling cycle; details can be found in Ref. [19].

Aging was monitored before and after the annealing by measuring the sample resistance at room temperature vs. time, with all samples stored in room air. Representative results are shown in Fig.1. The solid and dashed lines show the typical aging of non-annealed samples with and without plasma cleaning of the substrate, respectively. The two samples shown were fabricated in the same evaporation and oxidation step to ensure identical conditions. It is clear that plasma cleaning of the substrate before Al deposition results in significant reduction of aging, but does not stabilize the junctions. We conclude that some organic contaminants, most likely resist

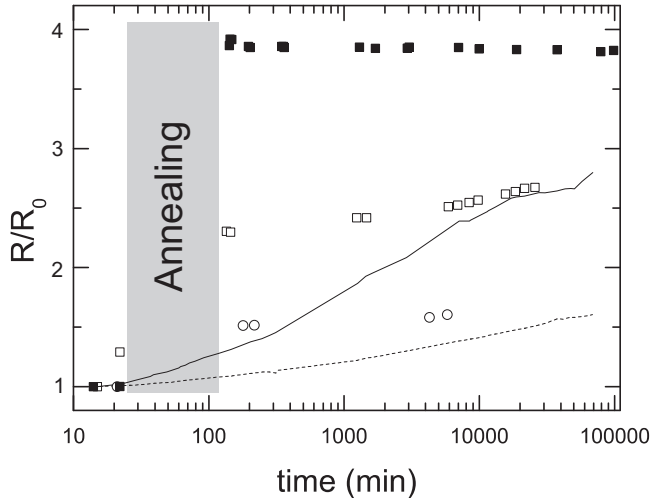


FIG. 1: Aging of a non-annealed sample with (dashed) and without (solid) plasma cleaning of the substrate. Open circles represent aging when the sample was annealed at 200°C, open squares at 300°C and filled squares at 400°C, respectively. All resistances are normalized with initial resistance at time equals zero (R_0).

residue on the substrate, are partly responsible for the aging phenomenon. The aging for a few representative annealed samples is also shown in Fig. 1, with different symbols denoting different annealing temperatures. The annealing process started approximately 20 minutes after the end of fabrication, which defines the zero of time and the initial resistance $R_0 = R(t = 0)$ for each sample. Clearly, annealing temperatures 200°C and 300°C do not lead to stabilization, whereas complete stabilization occurs at 400°C. Note that the last datapoints correspond to times over two months after the fabrication. Complete stabilization was also observed at annealing temperatures 350°C and 450°C (data not shown), but 500°C always resulted in breakdown of the junctions. In addition, the thermal treatments always led to increase of the sample resistance. At 400°C, where we have the largest amount of data (120 samples), the increase varied from a factor of two to a factor of eight, typically being between a factor of two to four. The range of initial R_T /junction for the 400°C treatments was from 1 kΩ to 100 kΩ, and no clear dependence of the R_T increase on the initial R_T was observed. Curiously, the low temperature anneals at 200°C and 300°C that did not lead to stabilization show approximately the same logarithmic aging rate as the non-annealed samples, see Fig. 1, but with a jump of the resistance caused by the treatment. This means that some of the resistance increase is not correlated with the stabilization in any way.

For ten two junction samples, the normal state tunneling properties were characterized before and after the annealing at 400°C by measuring the tunneling current and differential conductance dI/dV vs. bias voltage at 4.2 K with standard lock-in techniques. In this case, the

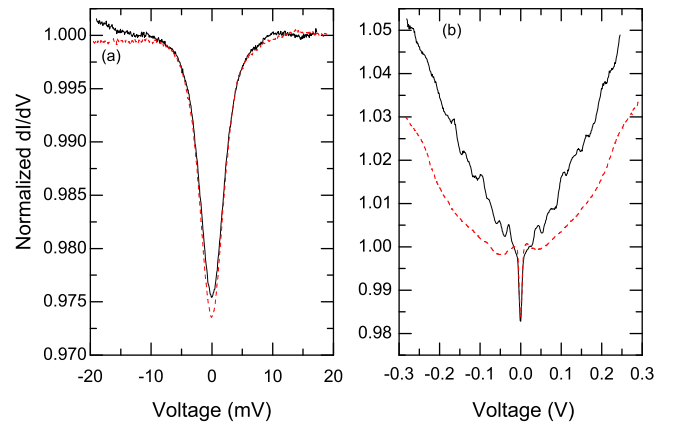


FIG. 2: (Color online) A typical normalized dI/dV vs. V spectrum in units of G_T of a sample before (solid) and after (dashed, red) annealing. (a) shows a narrow bias range focusing on Coulomb blockade, while (b) displays a wide bias voltage range (tunneling spectrum).

low bias voltage regime ($|V| < 20$ mV) provides information on the charging energy, i.e. capacitance, of the junctions. The charging energy $E_C = e^2/(2C_\Sigma)$, where C_Σ is total capacitance of the junctions and the island, can be obtained from the height of the zero-bias Coulomb blockade (CB) dip of dI/dV [Fig. 2 (a)] when $k_B T \gg E_C$, which is the appropriate limit for our junctions at 4.2 K. For two junctions in series, the height of the dip ΔG and E_C are related by $\Delta G/G_T = E_C/(6k_B T)$ [3], where G_T is the tunneling conductance around $V = 0$ without the CB dip. Figure 2 (a) shows a typical CB dip in our samples before and after the annealing. Usually E_C increased by 5 – 10 % after the annealing, with initial E_{CS} ranging from 9.8 μeV to 53 μeV corresponding to capacitances $C_\Sigma = 8.2$ –1.5 fF. The values of $R_T = 1/G_T$ increased 1.5–3 times for these samples after the annealing, varying initially from sample to sample between 9.5 kΩ and 151 kΩ.

In Fig. 2 (b) we plot a typical tunneling conductance spectrum (dI/dV) in a wide voltage bias range $|V| < 300$ mV. The spectrum shows many resonances (peaks) before the annealing, indicating that initially our barriers are far from perfect. These resonances are usually caused by unwanted impurities within the barrier, allowing inelastic or resonant tunneling at some specific energies [20]. Almost all resonances have clearly disappeared after the annealing treatment, in addition the strength of the voltage dependence has been reduced. One possibility discussed before [12] is that aluminum hydrates present in the disordered barriers dehydrate in the annealing, causing the resonances due to O-H groups to disappear. In an idealized case, i.e. by assuming a trapezoidal barrier and that direct tunneling dominates, the voltage dependence of the tunneling conductance is commonly parametrized in the WKB approximation as $G = G_0[1 + (V/V_0)^2]$, where $V_0^2 = 4\hbar^2\phi_0/(e^2md^2)$ and $G_0 = e^2 A \sqrt{2m\phi_0}/(\hbar^2 d) \exp(-2d\sqrt{2m\phi_0}/\hbar)$. Here

A is the junction area, ϕ_0 is the average barrier height and $d = (m^*/m)^{1/2}d_{ox}$ is the effective barrier thickness, where d_{ox} is the physical thickness and m^* the barrier effective mass. [20] Within this model we conclude that the curvature parameter V_0 increases in the annealing treatment. Together with the increase of E_C and R_T we can deduce that both the barrier height ϕ_0 as well as its effective thickness d increase with the annealing treatment. We stress that the increase of E_C alone (decrease of C_Σ) does not guarantee that d increases, as the dielectric constant most definitely also changes during the annealing. Similar kind of changes in junction parameters have also been reported earlier at least for gas annealed Nb/Al-AlO_x-Nb junctions [13, 15]. The change in the absolute values of the barrier parameters are difficult to estimate, as the numerous resonances in the conductance spectrum before the annealing makes fitting to the model unreliable. Quadratic fit to the annealed data yields the values $d = 9.5$ Å and $\phi_0 = 1.6$ eV for the sample in Fig. 2.

In addition to the improved tunneling characteristics, we also observed an improvement in the Al film quality by the treatments. This was checked by measuring the resistance of a 70 nm thick, 550 nm wide wire sample at 4.2 K before and after annealing at 400°C. The resistivity decreased by $\sim 30\%$ from 5.1 to $3.4 \mu\Omega\text{cm}$, corresponding to an increase in mean free path from 7.7 nm to 12 nm. High resolution SEM images of the film were also taken before and after the annealing, without any noticeable difference in the film grain structure.

In addition to measurements at 4.2 K, we also determined the superconducting properties of six unshunted single junction samples, cooled to below 100 mK in a dilution refrigerator. A representative I-V characteristic before and after annealing at 400°C is presented in Fig 3 (a). The increase of R_T is apparent as the decrease of the slope at high bias, in this sample approximately a factor of three. The superconducting gap Δ was determined from the curves, with the maxima of the dI/dV giving 2Δ , whose value did not change after the annealing. Reduction of the critical current I_C around zero bias is also visible, as expected from the Ambegaogar-Baratoff relation, [2] where $I_C R_T = \text{const}$ for a constant $\Delta =$. To study the supercurrent branch more accurately, we measured the switching currents by the cumulative histogram method, where a set of current pulses of constant height I_p were fed through the sample at a frequency 100 Hz and a duty cycle 5 %, and the time dependent voltage response was measured. By counting how often the junction switched to the finite voltage state at a particular I_p , the switching probability distribution of the sample is directly determined. Fig. 3 (b) shows the obtained results for the sample whose IV data is shown in Fig. 3 (a). It is clear that the switching current I_S (defined as the value where the probability = 0.5) is reduced to approximately one fifth of the initial value, while the width of the distribution also decreases.

By calculating the fluctuation free critical current I_C

from the Ambegaogar-Baratoff relation and estimating

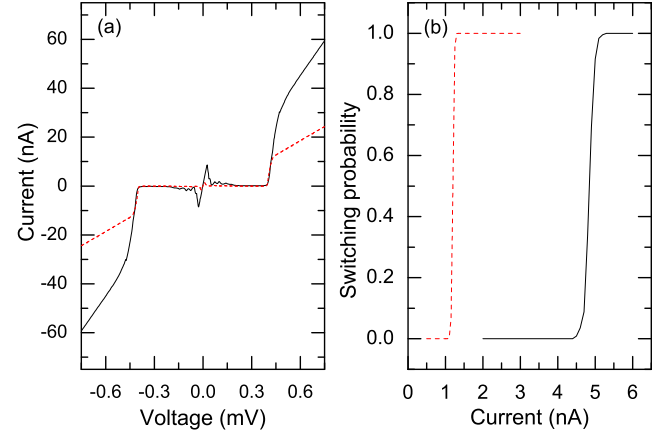


FIG. 3: (Color online) (a) Typical IV curve and (b) switching probability characteristics of a superconducting single junction sample before (solid) and after (dashed, red) annealing measured at 80 mK.

the capacitance of the junction as half of the capacitance measured for the two junction samples of the same junction size, the ratio of the Josephson coupling energy E_J and the charging energy E_C can be estimated to be $E_J/E_C \sim 1.8$. This means that the samples are in the underdamped regime, where for unshunted junctions the prediction is that $I_S \propto R_T^{-3/2}$. [21] The size of reduction in the switching current I_S is therefore fully consistent with the increase in R_T .

In conclusion, Al-AlO_x-Al tunnel junctions can be completely stabilized against aging by vacuum annealing at 350 – 450°C. This is an obvious advantage, when considering practical and commercial applications of tunnel junction devices. The improvement of the tunneling characteristics was also apparent as unwanted resonances disappeared after the treatment. Annealing led to a consistent reduction of junction capacitance and tunneling conductance for all samples studied, caused by an increase in the barrier height and thickness. Engineering these sample parameters in a controlled way by thermal vacuum annealing was not yet possible, partly because the microscopic understanding of the processes taking place is unclear. One possible application for the annealing is to increase the sensitivity of Josephson junction threshold current detectors, currently used for example in superconducting quantum bit readouts [6] or in shot-noise measurements. [22] With annealing, a reduction of the critical current can be achieved without a significant reduction of the capacitance, which decreases the sensitivity. [23]

We thank J. Männik for discussions. This work has been supported by the Academy of Finland projects No. 105258 and 205476 (TULE program). P.J.K. acknowledges National Graduate School in Materials Physics and Emil Aaltonen Foundation for partial financial support.

[1] C. Enss, ed., *Cryogenic Particle Detection* (Springer, 2005).

[2] H. Grabert and M. Devoret, eds., *Single Charge Tunneling: Coulomb Blockade Phenomena In Nanostructures*, NATO ASI Series (Plenum, New York, 1992).

[3] F. Giazotto, T. T. Heikkilä, A. Luukanen, A. M. Savin, and J. P. Pekola, *Rev. Mod. Phys.* **78**, 217 (2006).

[4] R. McDermott, R. W. Simmonds, M. Steffen, K. B. Cooper, K. Cicak, K. D. Osborn, S. Oh, D. P. Pappas, and J. M. Martinis, *Science* **307**, 1299 (2005).

[5] T. Yamamoto, Y. A. Pashkin, O. Astafiev, Y. Nakamura, and J. S. Tsai, *Nature* **425**, 941 (2003).

[6] A. A. D. Vion, A. Cottet, P. Joyez, H. Pothier, C. Urbina, D. Esteve, and M. H. Devoret, *Science* **296**, 886 (2002).

[7] I. Chiorescu, Y. Nakamura, C. J. P. M. Harmans, and J. E. Mooij, *Science* **299**, 1869 (2003).

[8] A. Wallraff, D. I. Schuster, A. Blais, L. Frunzio, J. Majer, M. H. Devoret, S. M. Girvin, and R. J. Schoelkopf, *Phys. Rev. Lett.* **95**, 060501 (2005).

[9] J. S. Moodera, L. R. Kinder, T. M. Wong, and R. Meservey, *Phys. Rev. Lett.* **74**, 3273 (1995).

[10] M. Nahum and J. Martinis, *Appl. Phys. Lett.* **63**, 3075 (1993).

[11] E. Tan, P. G. Mather, A. C. Perrella, J. C. Read, and R. A. Buhrman, *Phys. Rev. B* **71**, 161401(R) (2005).

[12] J. V. Gates, M. A. Washington, and M. Gurvitch, *J. Appl. Phys.* **55**, 1419 (1984).

[13] T. Lehnert, D. Billon, C. Grassl, and K. H. Gundlach, *J. Appl. Phys.* **72**, 3165 (1992).

[14] A. Oliva and R. Monaco, *IEEE Trans. Appl. Supercond.* **4**, 25 (1994).

[15] E. Cimpoiasu, S. Tolpygo, X. Liu, N. Simonian, J. Lukens, K. Likharev, R. Klie, and Y. Zhu, *J. Appl. Phys.* **96**, 1088 (2004).

[16] R. C. Sousa, J. J. Sun, V. Soares, P. P. Freitas, A. Kling, M. da Silva, and J. Soares, *Appl. Phys. Lett.* **73**, 3288 (1998).

[17] R. Wang, X. Jiang, R. M. Shelby, R. M. Macfarlane, S. S. P. Parkin, S. R. Bank, and J. S. Harris, *Appl. Phys. Lett.* **86**, 052901 (2005).

[18] H. Scherer, T. Weimann, A. B. Zorin, and J. Niemeyer, *J. Appl. Phys.* **90**, 2528 (2001).

[19] P. J. Koppinen, L. M. Väistö, and I.J.Maasilta, *AIP Conf. Proc.* **850**, 1639 (2006).

[20] E. L. Wolf, *Principles of Electron Tunneling Spectroscopy* (Oxford University Press, 1985).

[21] P. Joyez, P. Lafarge, A. Filipe, D. Esteve, and M. Devoret, *Phys. Rev. Lett.* **72**, 2458 (1994).

[22] J. P. Pekola, T. E. Nieminen, M. Meschke, J. M. Kivioja, A. O. Niskanen, and J. J. Vartiainen, *Phys. Rev. Lett.* **95**, 197004 (2005).

[23] J. M. Kivioja, T. E. Nieminen, J. Claudon, O. Buisson, F. W. J. Hekking, and J. P. Pekola, *New J. Phys.* **7**, 179 (2005).